ORIGINAL ARTICLE

WILEY

Circ_0003340 downregulation mitigates esophageal squamous cell carcinoma progression by targeting miR-940/PRKAA1 axis

Xingzhuo Guan | Xiaohui Guan | Yuanshi Wang | Tingzhu Lan | Tongshuang Cheng | Yan Cui | Hongjun Xu 🔵

Department of Gastroenterology, Affiliated
Hospital of Beihua University, Jilin City, China

Correspondence
Hongjun Xu, Department of Gastroenterology,
Affiliated Hospital of Beihua University, No.12
Liberatterion Middle Road, Chuanying District,
Jilin 132000, Jilin Province, China.
Email: xuhongjun73117@163.com

Abstract

Background: Esophageal squamous cell carcinoma (ESCC) is a highly prevalent type of esophageal cancer (EC), usually found at an advanced stage with a high mortality rate, and it is now crucial to find new ways to diagnose and treat ESCC. This study analyzed the function of circular RNA_0003340 (circ_0003340)/microRNA-940 (miR-940)/protein kinase AMP-activated alpha 1 catalytic subunit (PRKAA1) axis in ESCC.
Methods: Circ_0003340, miR-940 and PRKAA1 contents were measured with the application of real-time quantitative polymerase chain reaction (RT-qPCR) and western blot. Cell proliferation, cell cycle, apoptosis, migration, invasion and angiogenesis were assessed with a cell counting kit-8 (CCK8), 5-ethynyl-2′-deoxyuridine (EdU), flow cytometry, wound healing, transwell and tube formation assays. We used both the luciferase reporter system and RNA immunoprecipitation (RIP) to analyze the relationship between miR-940 and circ_0003340 or PRKAA1. Finally, xenograft models were applied to analyze the effect of circ_0003340 on tumor growth in vivo.
Results: Upregulated circ_0003340 and PRKAA1, and downregulated miR-940 levels were detected in ESCC. Meanwhile, ESCC progression was apparently restrained by circ_0003340 knockdown in vitro. Circ_0003340 acted as a ceRNA for miR-940 in regulating ESCC progression and miR-940 was proved to target PRKAA1 to arrest ESCC progression in vitro. Finally, in vivo experiments established that silencing of circ_0003340 slowed tumor growth in vivo.
Conclusion: Circ_0003340 downregulation mitigated esophageal squamous cell carcinoma progression by targeting miR-940/PRKAA1 axis.

KEYWORDS
circ_0003340, ESCC, miR-940, PRKAA1

INTRODUCTION

Esophageal cancer has been reported to be the seventh cause of cancer death worldwide in recent research studies.[1] Esophageal squamous cell carcinoma (ESCC) is the leading category of EC, with approximately 90% of EC patients diagnosed with ESCC and a smaller proportion with adenocarcinoma (EADC).[2] Causes of ESCC may include smoking, alcoholic beverage intake, low vegetable and fruit intake,

etc.[3] ESCC has no obvious symptoms in the early stages and is usually detected in the late stages. The advanced stage of ESCC is characterized by high metastasis, widespread drug resistance, and high recurrence rates,[4] the five-year survival rates for ESCC remain below 20% in developed countries and below 5% in developing countries.[5] Although medical advances in the treatment of ESCC have been remarkable, they have only improved the survival rate of patients with ESCC in the early stages, so seeking ways for early diagnosis of ESCC is important to improve ESCC patient survival. The combination of endoscopic resection surgery and

---

Xingzhuo Guan and Xiaohui Guan contributed equally to this paper.

chemotherapy is mainly used in the early stage of ESCC, which has significantly improved the survival rate of ESCC patients. In the late stage, multiple chemotherapeutic drugs are usually used for treatment, whereas the survival rate of patients is still unsatisfactory,[6] but the recent advent of immunotherapy molecular therapy brings great hope for the treatment of advanced ESCC.

Circular RNAs (circRNAs), initially found in viruses, were thought to be the product of exon splicing errors and to have no biological function,[7] but as research has progressed, some circRNAs have been found in mammalian cells with abundant expression, conserved and endogenous characteristics, and the ability to regulate various types of physiological or pathological activities.[8] At the same time, circRNAs possess a higher stability compared to corresponding linear RNAs, which may be due to their closed-loop structure, and this supports the potential of circRNAs as disease diagnostic markers.[9] In various types of diseases, accumulated data revealed the differentially expressed circRNAs, especially in various types of cancer. In lung cancer, circ-CPA4 was examined in high abundance, and silencing of circ-CPA4 blocked cancer cell proliferation and epithelial mesenchymal transition, but increased apoptosis and enhanced cisplatin resistance by sponging let-7 miRNA.[10] Guo et al. demonstrated that circ_0023404 targeted miR-5047 to boost the metastasis of cervical cancer cells and exacerbate cisplatin resistance.[11] Circ_0044516 was also proved to be highly upregulated in prostate cancer (PC) tissues and exosomes. Silencing of circ_0044516 apparently slowed down the proliferation and metastasis of PC cells, showing that circ_0044516 acted as an oncogene in PC.[12] Circ_0003340 was found to be dysregulated in ESCC and regulated ESCC progression in vitro, but the regulatory mechanism of circ_0003340 in ESCC is still not thoroughly investigated.[13] Our study further analyzed the regulatory network of circ_0003340 in ESCC.

MicroRNAs (miRNAs) are a class of non-coding RNAs with small molecular structures that negatively regulate the expression of downstream genes.[14] MiRNAs are involved in regulating cellular processes such as cell proliferation, differentiation and apoptosis.[15] In several studies, miRNAs were found to act on the 3′untranslated region (3′UTR) of target genes to regulate their levels, which in turn regulated related biological processes, and a large number of miRNAs were found in various diseases.[16–18] For example, miR-193a has been widely studied in various types of cancer and can play different roles in different cancers. It has been identified that miR-193a acts as a tumor-suppressor factor in colon cancer,[17] and miR-193a promotes cancer cell migration, invasion and mesenchymal transition by targeting BTRC in glioma.[18] MiR-193a level has also been confirmed to be associated with patient survival, cancer staging and chemoresistance.[16] Furthermore, many miRNAs have been observed to be dysregulated in cancer, such as miR-940, which was previously reported to be dysregulated in ESCC.[19] Our study further analyzed the function and action mechanism of miR-940 in ESCC.

The protein kinase AMP-activated alpha 1 catalytic subunit (PRKAA1, also known as AMPK alpha 1), is an important member of the serine/threonine protein family, and is involved in pathways including lipid metabolism and gluconeogenesis, and has a regulatory role in energy level in cells.[20] PRKAA1 is an important catalytic unit in AMPK, which has been shown to be widely involved in cancer-related pathways by affecting cellular processes such as cell proliferation, differentiation and apoptosis.[21] Zhang et al. identified that high abundance of PRKAA1 was correlated with poorer survival in gastric cancer (GC) tissues, and PRKAA1 knockdown markedly repressed GC cell migration and invasion.[22] In this study, we analyzed the action mechanism of circ_0003340/miR-940/PRKAA1 in ESCC.

METHODS

Tissue samples

All projects of this institute were endorsed by the Affiliated Hospital of Beihua University. With the consent of 45 patients diagnosed with ESCC at Affiliated Hospital of Beihua University, the corresponding cancerous and paraneoplastic tissues were collected and tested. All patients were untreated and tumor stage and presence of lymph node metastasis were diagnosed under uniform criteria. Written consent forms were collected from all participants.

Cell culture and transfection

Esophageal epithelial cells HET-1A and ESCC cells (Eca-109 and TE-1) were purchased from Chuan Qiu Biotechnology (Shanghai, China) and grown in DMEM medium (Genetimes) with 10% FBS (Genetimes). All culture dishes were placed at 37°C with 5% CO_2. The small interfering RNA (siRNA) of circ_0003340 (si-circ_0003340), short hairpin RNA (shRNA) of circ_0003340 (sh-circ_0003340), pCD-ciR-circ_0003340, miR-940 mimic (miR-940), miR-940 inhibitor (anti-miR-940), pcDNA-PRKAA1 (PRKAA1) and the corresponding controls (NC) including si-NC, sh-NC, empty pCD-ciR and pcDNA, miR-NC, and anti-miR-NC were synthesized by GenePharma and transfected into Eca-109 and TE-1 cells under the application of Lipofectamine 2000 (Invitrogen) in compliance with the manufacturer's instructions.

RNA extraction and real-time quantitative polymerase chain reaction (RT-qPCR)

Total RNA was isolated using TRIzol (Invitrogen) as per the manufacturer's instructions and nucleoplasmic separation assays were conducted using a nuclear/cytosol fractionation kit (Solarbio). Subsequently, cDNA was synthesized according to the instructions of the miScript RT Kit

(TaKaRa). SYBR Green (TaKaRa) was deployed to execute RT-qPCR, and the resulting data were analyzed with GAPDH and U6 as internal reference according to $2^{-\Delta\Delta CT}$ method. Specific primer information is listed in Table 1.

Proliferation analysis

The cell counting kit-8 (Dojindo,) was utilized to evaluate the proliferation of ESCC cells. The transfected cells were inoculated in 96-well plates, and then 10 μl of the CCK8 solution was added at 24, 48 and 72 h, respectively, and the cells continued to be cultured for 4 h before the absorbance was detected at 450 nm.

5-ethynyl-2′-deoxyuridine (EdU) assay was also employed in the assessment of ESCC cell proliferation. In this study, a Yefluor 488 EdU Imaging Kit (Yeasen) was used for analysis. ESCC cells were cultured in a 96-well plate for 24 h. Then, the cells were incubated with EdU solution for 2 h. After the cells were fixed and stained with the nuclear dye DAPI for 30 min in the dark, the proliferation capacity was then observed and analyzed under the microscope.

Cell cycle and apoptosis analysis

ESCC cell cycle distribution and apoptosis were evaluated with cell cycle assay kit (Beyotime) and Annexin V-fluorescein isothiocyanate (FITC) cell apoptosis detection kit (Beyotime), coupled with flow cytometry analysis. In brief, the working solution of propidium iodide (PI) staining buffer supplemented with RNase A was incubated with the cells to stain DNA, and thus cells distributed in different cell cycle phases were detected under the application of flow cytometer. For cell apoptosis analysis, the cells were incubated in the Annexin V-FITC binding buffer containing Annexin V-FITC and PI reagents, and then Annexin V-FITC and/or PI signals were detected under the application of flow cytometer.

TABLE 1 Primer sequences used for RT-qPCR

Name		Primers for PCR (5′-3′)
hsa_circ_0003340	Forward	CGTGCCCGCTGACATTATCT
	Reverse	GGGGAAGGGGACTCTGGTAG
PRKAA1	Forward	AAAACAGGCTCCACGAAGGA
	Reverse	CATGTGTGCATCAAGCAGGAC
miR-940	Forward	GCCGAGAAGGCAGGGCCCCCG
	Reverse	CTCAACTGGTGTCGTGGAG
GAPDH	Forward	GACAGTCAGCCGCATCTTCT
	Reverse	GCGCCCAATACGACCAAATC
U6	Forward	CTCGCTTCGGCAGCACA
	Reverse	AACGCTTCACGAATTTGCGT
OGDH	Forward	CTGGTAGAAGCACAGCCCAA
	Reverse	GTCCAGCTGTGCTACATGGT

Western blot

First, RIPA (Beyotime) was utilized for protein extraction, and protein quantification was carried out following the procedure of the BCA Protein Assay Kit (Beyotime). Then, 1 μg of protein was subjected to western blot as described in Hong et al.[10] The proteins were separated using sodium dodecyl sulfate-polyacrylamide gel electrophoresis, and then transferred onto the PVDF membranes (Beyotime). Later, the membranes were blocked with 5% skimmed milk, and then incubated with primary and secondary antibodies. The eyoECL Plus Kit (Beyotime) was employed to detect protein signals on the membrane and ImageJ software (NIH) was used to measure protein expression levels with normalization to GAPDH. All antibodies including anti-PCNA (ab92552, 1/10000, Abcam), anticyclin D1 (ab16663, 1/200, Abcam), anticleaved caspase 3 (ab32042, 1/500, Abcam), anti-GAPDH (ab22555, 1/5000, Abcam) and anti-PRKAA1 (ab32047, 1/5000, Abcam), as well as horseradish peroxidase (HRP)-conjugated secondary (ab205718, 1/50000, Abcam) were obtained from Abcam.

Caspase-3 activity analysis

Caspase-3 activity was analyzed under the application of Caspase-3 activity assay kit (ab252897, Abcam). Cells were lysed in the Caspase cell lysis buffer, and the supernatant of the lysate was incubated with the mixture of Caspase reaction buffer, Ac-DEVD-AFC and DTT. Eventually, the fluorescence was immediately measured at Ex/Em = 400/505 nm by a microplate reader. The activity was calculated according to the AFC standard curve, which was plotted beforehand.

Wound healing assay

Before the experiment started, marker lines were drawn on the outside of the culture dish. Then the transfected cells were evenly inoculated in the culture dish, and when the fusion reached about 90%, the cells at the delineation were exfoliated with a sterile toothpick, eluted and photographed, and the migration ability was analyzed by photographing again after continuing the culture for 24 h.

Transwell assay

Transwell chambers (Corning) precoated with matrigel matrix (Corning) were used to evaluate the invasion ability of ESCC cells. The upper chamber was supplemented with serum-free DMEM medium, while the lower chamber was supplemented with the medium containing 10% FBS. The upper chamber was inoculated with transfected cells for 24 h, then the cells which had invaded through the membrane were fixed with methanol and stained with crystal

violet and placed under a microscope for observation and analysis.

Tube formation assay

Matrigel matrix (Corning) was spread over the bottom of the cultured 96-well plates on ice and then fixed at 37°C. Human umbilical vein endothelial cells (HUVECs; Procell) were resuspended in conditioned medium from differently transfected ESCC cells and inoculated into 96-well plates with 2×10^4 cells per well. Five replicates were performed per condition, and HUVECs were cultured in the serum-free medium for 24 h, and the length and characteristics of vessel-like tubes, including the number of nodes or branchpoints, were photographed and analyzed by microscopy after 12 h.

Dual-luciferase reporter assay

The sequences of circ_0003340-wild type (circ_0003340 wt) and PRKAA1 3′UTR wt containing the miR-940 binding site were constructed into the psi-check2 vector to obtain the recombinant vector circ_0003340^{wt} and PRKAA1 3′UTR^{wt}. The circ_0003340-mutant type (circ_0003340 mut) and PRKAA1 3′UTR mut containing the mutations of miR-940 binding site were happened in the recombinant vector circ_0003340^{mut} and PRKAA1 3′UTR^{mut} based on the wt vectors. Subsequently, the luciferase reporter vectors were cotransfected with miR-940 mimic into ESCC cells for 48 h, and each group of luciferase activity was assessed under the application of the dual luciferase reporter assay kit (Promega).

RNA immunoprecipitation (RIP) assay

RIP assay was used to measure the interaction relationship among circ_0003340, miR-940 and PRKAA1 using the EZ-Magna RIP RNA-binding protein immunoprecipitation kit (Millipore). Cells were lysed and placed in RIP buffer, and incubated with magnetic beads coupled with Ago2 antibody or IgG antibody. The mixture was then cocultured with protease K to decompose the protein content, and immunoprecipitated RNA was purified from the complex, and the levels of circ_0003340, miR-940 and PRKAA1 in the precipitates were detected by RT-qPCR.
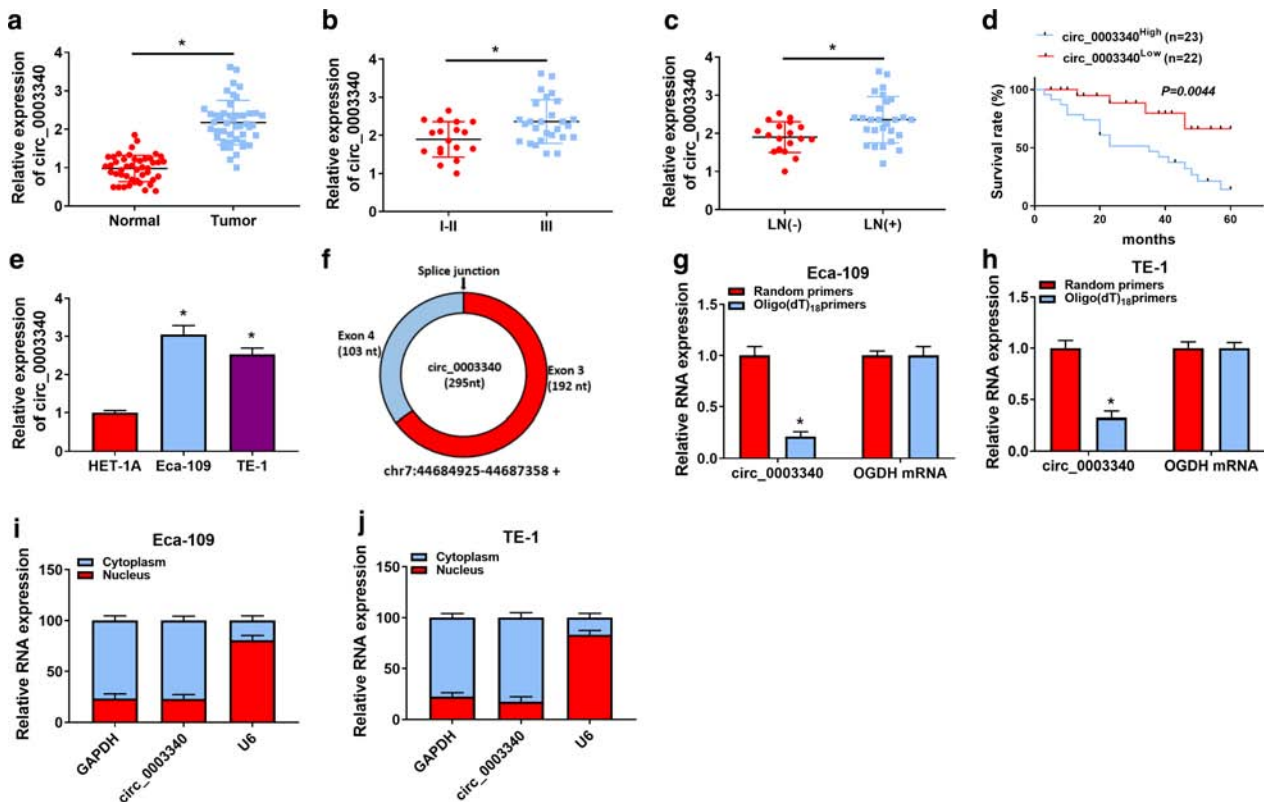

FIGURE 1 Expression characteristics of circ_0003340 in esophageal squamous cell carcinoma (ESCC). (a–c) The expression of circ_0003340 was detected by RT-qPCR in ESCC tumor and normal tissues, tumor node metastasis (TNM) I–II and III stages, and lymph node metastasis-negative (LN[−]) and lymph node metastasis-positive (LN[+]) tissues. (d) Survival curves of patients in circ_0003340^{high} and circ_000334^{low} groups were analyzed by log-rank test. (e) The expression of circ_0003340 in ESCC and normal cells was detected. (f) Circ_0003340 structure diagram is shown. (g and h) Reverse transcription PCR of circ_0003340 and OGDH using either oligo(dt)$_{18}$ primer or random primer. (i and j) The subcellular localization of circ_0003340 major expression sites were detected by nucleoplasmic segregation assay. *$p < 0.05$
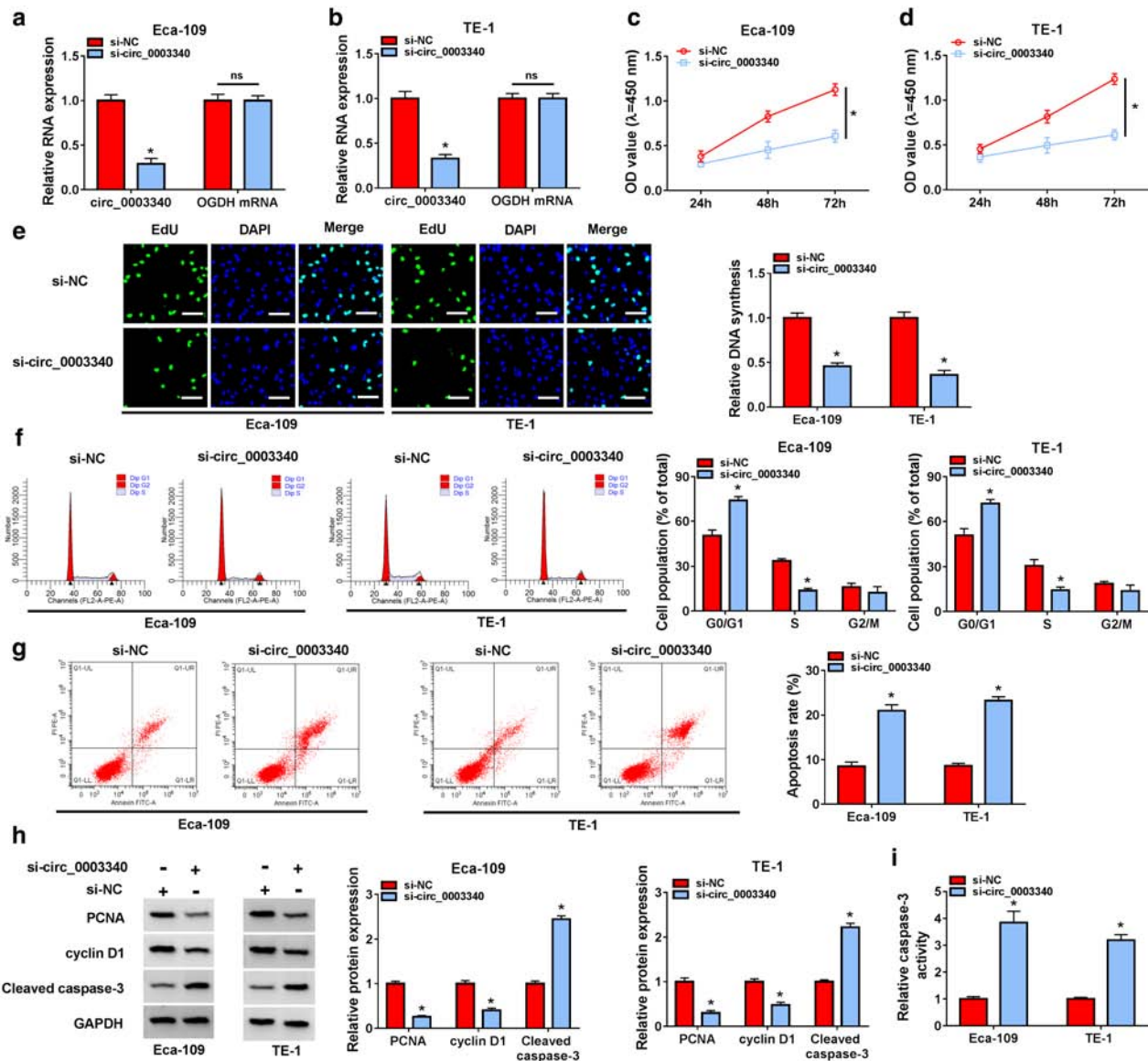
FIGURE 2 Circ_0003340 knockdown evidently blocked esophageal squamous cell carcinoma (ESCC) cell proliferation and induced cell cycle arrest and apoptosis. (a and b) The knockdown efficiency of si-circ_0003340 was analyzed by RT-qPCR. Si-circ_0003340 was transfected into Eca-109 and TE-1 cells, (c and d) CCK8 was applied to assess ESCC cell viability, (e) EdU assay was performed to detect cell proliferation, (f and g) flow cytometry was used to detect the cell cycle and apoptosis, (h) western blotting was launched to assess PCNA, cyclin D1 and cleaved caspase 3 protein levels, and (i) caspase-3 activity assay kit was utilized to measure caspase-3 activity. $*p < 0.05$

Xenograft models

The experiment in mice was approved by the Animal Care Committee of Affiliated Hospital of Beihua University. Ten 6-week-old BALB/c nude mice purchased from Vital River Laboratory Animal Technology Co., Ltd. (Beijing, China) were randomly divided into two groups and injected with Eca-109 cells stably transfected with sh-circ_0003340 or sh-NC, respectively. Tumor volumes (volume = width^2 × length × 0.5) were calculated weekly after injection, and all mice were euthanized after 4 weeks, and tumor tissues were collected and weighed for subsequent analysis. Xenograft tumor samples were fixed in 4% paraformaldehyde, embedded in paraffin and

sliced into 4 μm sections for immunohistochemistry (IHC) staining.

IHC assay

Endogenous peroxidase was blocked by hydrogen peroxide, and antigen retrieval was performed by heating in the microwave on band 3 for 10–15 min (700 W oven). The sections were subsequently incubated with anti-Ki67 (Abbkine) overnight at 4°C and HRP-conjugated secondary (ab205718, 1/10000, Abcam) for 2 h at room temperature. Finally, the staining processes were performed with DAB (DAB Kit,
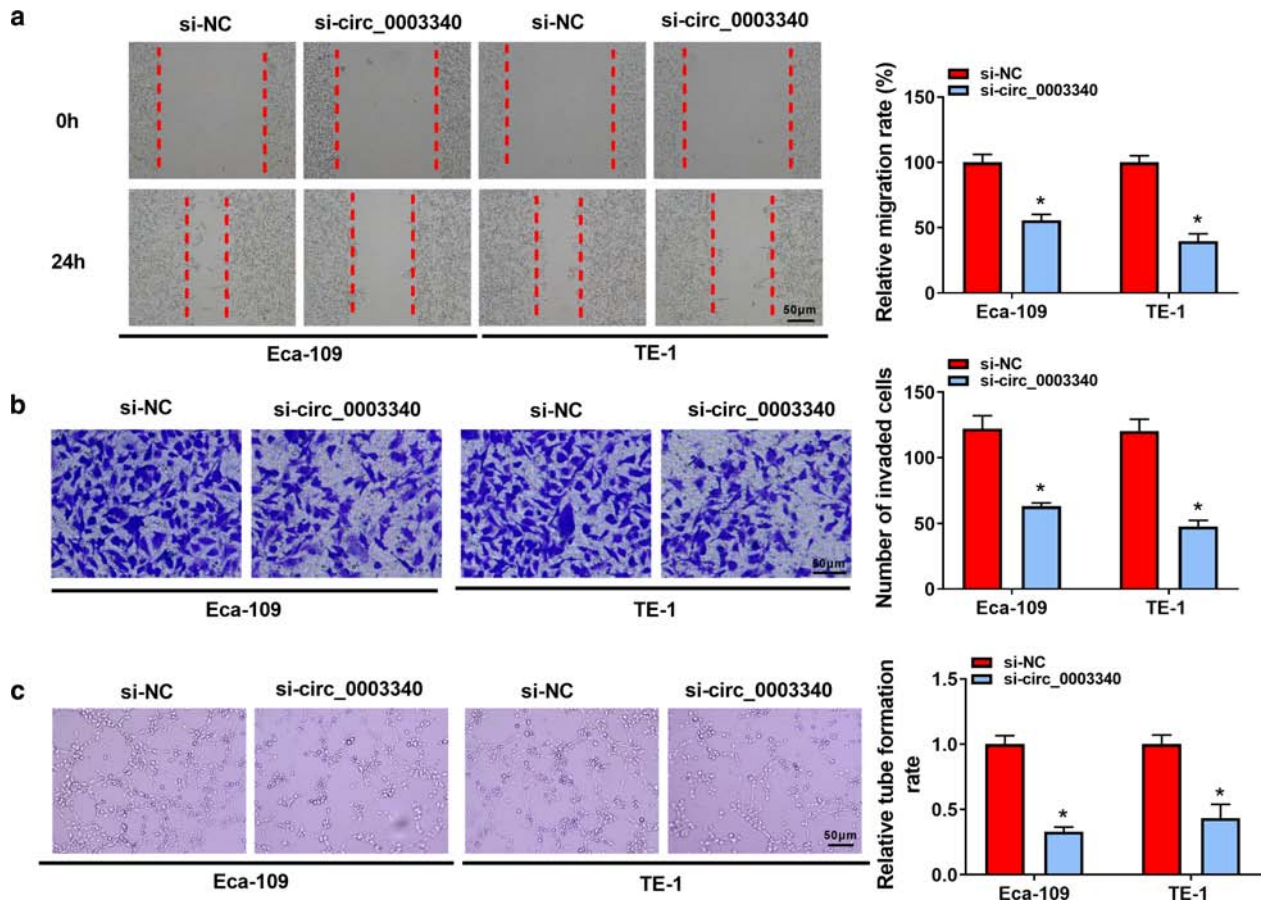
FIGURE 3 Effects of circ_0003340 downregulation on esophageal squamous cell carcinoma (ESCC) cell migration, invasion and angiogenesis. Si-circ_0003340 or si-NC was transfected into Eca-109 and TE-1 cells. (a) Wound healing assay was conducted to assess cell migration. (b) Transwell assay was performed to detect cell invasion. (c) Tube formation assay of HUVECs was conducted to evaluate angiogenesis. *$p < 0.05$

ZSGB-BIO, China) and hematoxylin (Sigma-Aldrich) at room temperature. The slices were then observed using a light microscopy (JEOL). Positive cell counts were performed using Japanese Nikon imaging analysis software, and three equal-area nonrepetitive fields ($\times 200$) were selected for each slice to calculate the number of positive cells.

Statistical analysis

SPSS 20.0 (IBM Corp.) was conducted to analyze the data, and differences between groups were assessed by Student's t-test or analysis of variance. p-value <0.05 was considered statistically significant.

RESULTS

Circ_0003340 was highly expressed in ESCC

RT-qPCR data revealed a higher abundance of circ_0003340 in ESCC tissues compared to normal tissues (Figure 1a), and circ_0003340 was also highly expressed in ESCC patients with advanced tumor stage (III) and positive lymph node metastasis (Figure 1b,c). Survival rate was reduced in the circ_0003340^{high} group ($n = 23$) relative to the circ_0003340^{low} group ($n = 22$), indicating that high expression of circ_0003340 is associated with poor prognosis of ESCC patients (Figure 1d). In addition, high abundance of circ_0003340 was also detected in ESCC cells compared to HET-1A cells (Figure 1e). The structure of circ_0003340 is shown in Figure 1f. The inability of the Oligo(dt)$_{18}$ primer to amplify circ_0003340 also further supported the ring structure of circ_0003340 (Figure 1g,h). The nucleoplasmic separation assay revealed that circ_0003340 was mainly located in the cytoplasm (Figure 1i,j).

Progression of ESCC was markedly inhibited by silencing of circ_0003340 in vitro

RT-qPCR analysis uncovered the efficient knockdown of circ_0003340 in Eca-109 and TE-1 cells with si-circ_0003340 transfection (Figure 2a). The phenomenon of inhibition of Eca-109 and TE-1 cell proliferation induced by circ_0003340 downregulation was observed based on CCK8 and EdU data (Figure 2c–e). Flow cytometry analysis also indicated that si-circ_0003340 greatly arrested the cell cycle
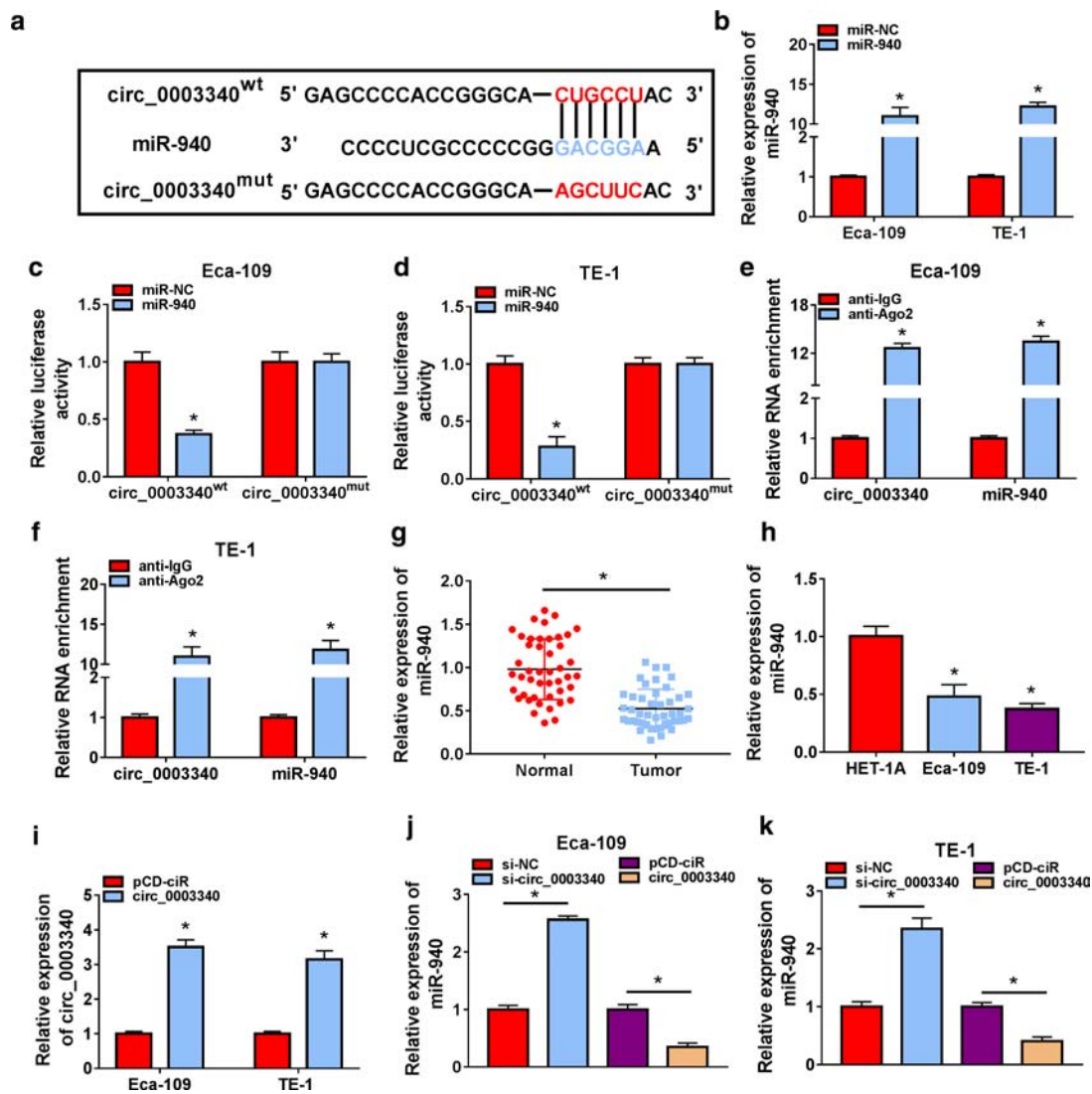
FIGURE 4 Validation of the relationship between circ_0003340 and miR-940. (a) The binding sites between circ_0003340 and miR-940 are shown. (b) Overexpression efficiency of miR-940 was assessed in Eca-109 and TE-1 cells by RT-qPCR. (c and d) Analysis of the relationship between circ_0003340 and miR-940 by luciferase reporter system in Eca-109 and TE-1 cells cotransfected with circ_0003340$^{wt/mut}$ and miR-940 or miR-NC mimic. (e and f) RIP assay was conducted to detect the enrichment of circ_0003340 and miR-940 in Ago2-immunoprecipitated complex, normalized to the IgG-immunoprecipitated complex. (g and h) MiR-940 in ESCC tissues and cells was determined by RT-qPCR. (i) The upregulation efficiency of pcD-circ_0003340 was demonstrated in Eca-109 and TE-1 cells by RT-qPCR. (j and k) MiR-940 level was measured by RT-qPCR in Eca-109 and TE-1 cells transfected with si-NC, si-circ_0003340, pcD-ciR or pcD-circ_0003340. *$p < 0.05$

at G0/G1 phase and promoted apoptosis in Eca-109 and TE-1 cells (Figure 2f,g). Protein levels of proliferation marker protein PCNA and cell cycle protein cyclin D1 were also depressed by circ_0003340 knockdown, while protein level of proapoptotic protein cleaved caspase 3 and caspase-3 activity were upregulated in Eca-109 and TE-1 cells (Figure 2h,i). The migratory and invasive abilities of ESCC cells were also assessed under the application of wound healing and transwell assays, and the results showed that the migration and invasion of Eca-109 and TE-1 cells with si-circ_0003340 transfection were attenuated compared with cells with si-NC transfection (Figure 3a,b). Finally, the inhibitory effect of circ_0003340 silencing on the tube formation rate is also seen in Figure 3c. Altogether, silencing of circ_0003340 dramatically repressed the progression of ESCC in vitro.

Circ_0003340 served as a sponge for miR-940

In order to investigate the mechanism of circ_0003340 in ESCC, we analyzed the potential targets of circ_0003340 using starBase software, and miR-940 was one of them. The binding sites are presented in Figure 4a. The upregulation efficiency of miR-940 was demonstrated in Eca-109 and TE-1 cells (Figure 4b). Dual luciferase reporter system and
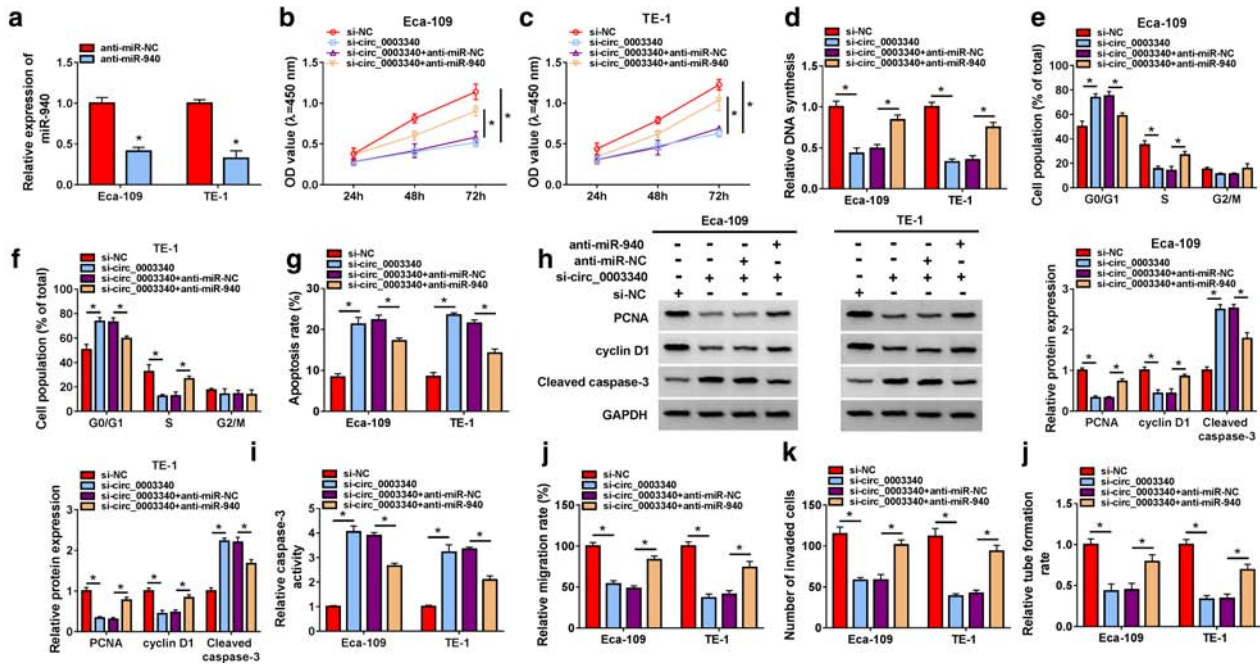
FIGURE 5 Circ_0003340 regulated esophageal squamous cell carcinoma (ESCC) progression by sponging miR-940 in vitro. (a) The transfection efficiency of anti-miR-940 are shown. Si-NC, si-circ_0003340, si-circ_0003340 + anti-miR-NC, si-circ_0003340 + anti-miR-940 were transfected into Eca-109 and TE-1 cells, (b–d) cell proliferation was measured using CCK8 and EdU assays. (e–g) Cell cycle and apoptosis were assessed by flow cytometry. (h–i) PCNA, cyclin D1 and cleaved caspase 3 protein levels and caspase-3 activity were tested by western blot and ELISA. (j and k) Cell migration and invasion were analyzed via wound healing and transwell assay. (l) Tube formation rate was detected. *$p < 0.05$

RIP assay were performed to verify the targeting relationship between circ_0003340 and miR-940, and the results showed that miR-940 mimic transfection in Eca-109 and TE-1 cells only considerably decreased the luciferase activity in the circ_0003340^wt group (Figure 4c,d). In the anti-Ago2 group, circ_0003340 and miR-940 were significantly enriched (Figure 4e,f), which suggested a direct targeting relationship between circ_0003340 and miR-940. Compared with normal tissues and HET-1A cells, miR-940 had lower abundance in ESCC tumor tissues, as well as in Eca-109 and TE-1 cells (Figure 4g,h). Meanwhile, RT-qPCR results revealed a promotion of miR-940 level by circ_0003340 downregulation via siRNA transfection and a reduction of miR-940 level caused by circ_0003340 overexpression mediated by the transfection of pcD-circ_0003340 plasmid (Figure 4i–k). The combined data suggested that miR-940 was a target of circ_0003340.

Knockdown of miR-940 weakened the inhibitory effect of circ_0003340 silencing on ESCC progression in vitro

As illustrated in Figure 5a, anti-miR-940 greatly reduced miR-940 level in Eca-109 and TE-1 cells. The suppressive effect of circ_0003340 downregulation on cell proliferation was overturned when Eca-109 and TE-1 cells were cotransfected with anti-miR-940 (Figures 5b–d), and circ_0003340 knockdown-induced cell cycle arrest and apoptosis were also

attenuated by miR-940 downregulation (Figures 5e–g). Meanwhile, miR-940 silencing diminished the effects of circ_0003340 downregulation on PCNA, cyclin D1 and cleaved caspase 3 protein levels and caspase-3 activity (Figure 5h,i). Finally, miR-940 knockdown returned the suppressive effects of si-circ_0003340 on migration, invasion and angiogenesis in Eca-109 and TE-1 cells (Figure 5j–l). All data showed that miR-940 knockdown abrogated the blocking effects of circ_0003340 silencing on ESCC progression in vitro.

MiR-940 targeted PRKAA1 in ESCC cells

According to StarBase software prediction, PRKAA1 is one of the candidate genes for miR-940, and the binding sites between them are shown in Figure 6a. The phenomenon that only the luciferase activity of the PRKAA1 3′UTR^wt group was downregulated with miR-940 cotransfection was revealed by dual luciferase reporter assay (Figure 6b,c). The remarkable enrichment of PRKAA1 and miR-940 by anti-Ago2 similarly supported the targeting relationship between PRKAA1 and miR-940 (Figure 6d,e). Subsequently, the higher abundance of PRKAA1 in tumor tissues and cells relative to normal tissues and cells was also unveiled by RT-qPCR and western blot (Figure 6f–h). Finally, the downregulation of PRKAA1 level by miR-940 transfection in Eca-109 and TE-1 cells and the promotion of PRKAA1 level by miR-940 knockdown are also illustrated in Figure 6i.
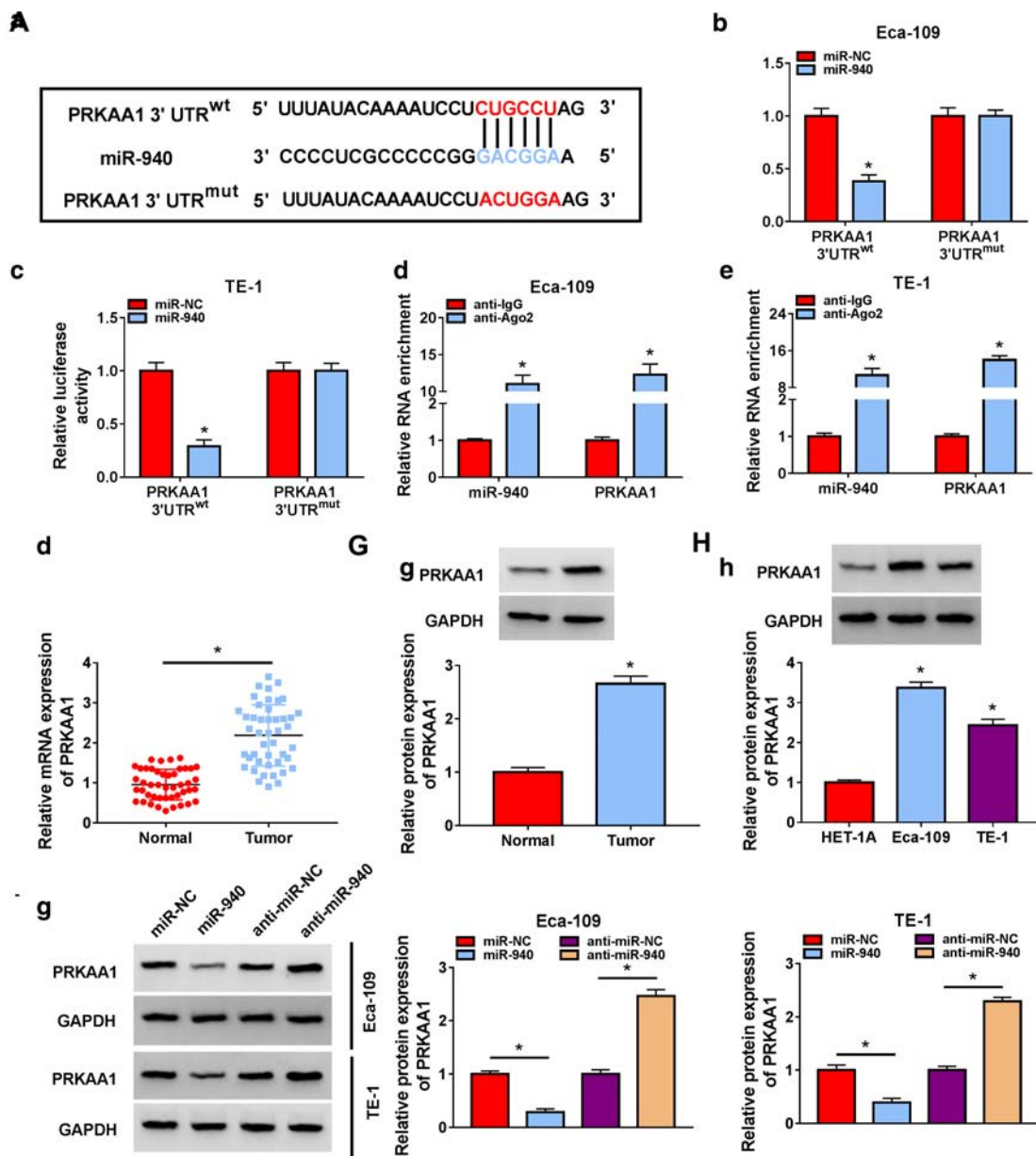
FIGURE 6 The association between miR-940 and PRKAA1 was verified. (a) Complementary binding sequences between miR-940 and PRKAA1 are shown. (b and c) The relationship between miR-940 and PRKAA1 was confirmed with the application of luciferase reporter system. (d and e) The relationship between miR-940 and PRKAA1 was confirmed with the application of RIP assay. (f–h) PRKAA1 content in ESCC tissues or cells was detected. (i) PRKAA1 protein level was analyzed by western blotting in Eca-109 and TE-1 cells transfected with miR-NC, miR-940, anti-miR-NC or anti-miR-940. *$p < 0.05$

MiR-940 targeted PRKAA1 to regulate ESCC progression in vitro

Ectopic expression of PRKAA1 in Eca-109 and TE-1 cells was induced by PRKAA1 overexpression vector transfection (Figure 7a). PRKAA1 overexpression overturned the suppression effect of miR-940 mimic on cell proliferation, as evidenced by the loss of cell viability and DNA synthesis (Figure 7b–d). Based on the results of flow cytometry, we observed that upregulation of PRKAA1 restored the effects of miR-940 mimic on cell cycle progression and apoptosis

(Figure 7e–g). Meanwhile, miR-940-mediated the impacts on PCNA, cyclin D1, cleaved caspase 3 protein levels and caspase-3 activity were abolished by PRKAA1 cotransfection (Figure 7h,i). In addition, upregulation of PRKAA1 recovered the suppression effects of miR-940 overexpression on migration, invasion and angiogenesis (Figure 7j–l). Finally, we also found that anti-miR-940 restored the inhibitory effect of circ_0003340 knockdown on PRKAA1 expression level (Figure 8a,b). Overall, circ_0003340 acted on the miR-940/PRKAA1 axis to modulate ESCC progression in vitro.
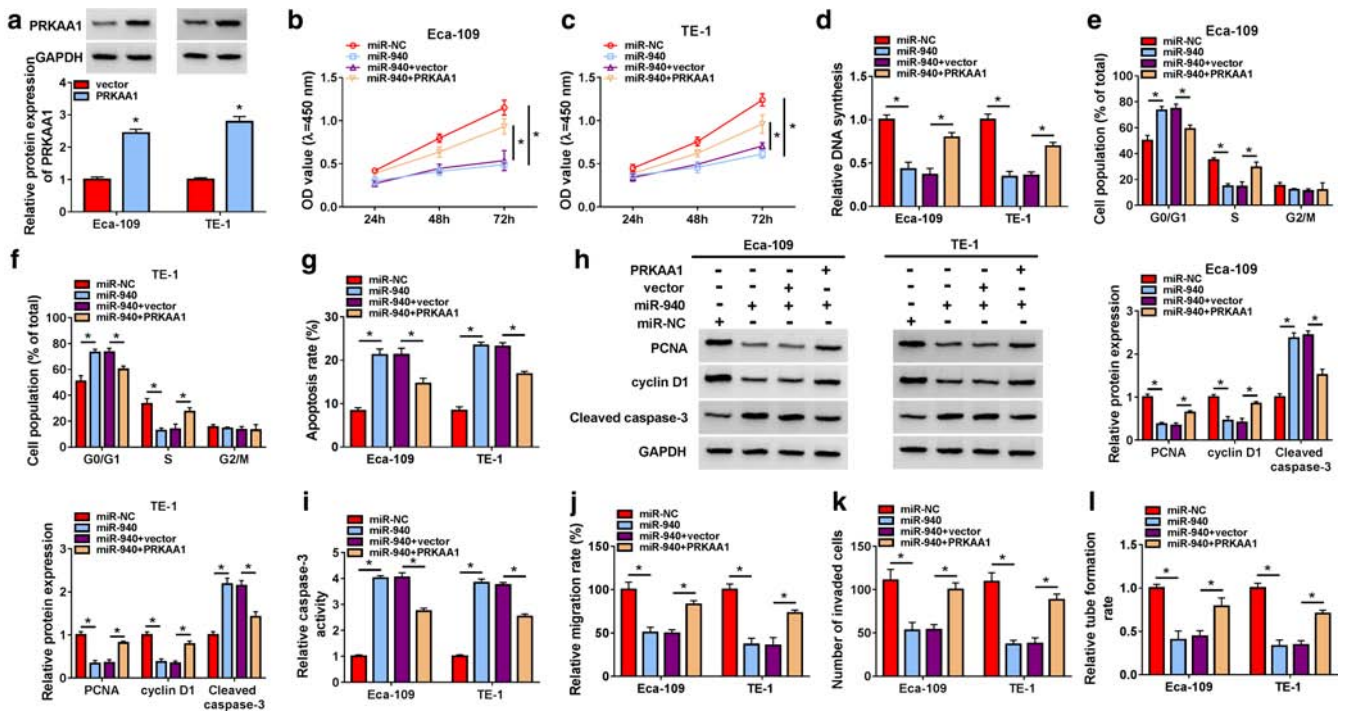
FIGURE 7 MiR-940 targeted PRKAA1 to regulate ESCC progression. (a) Overexpression efficiency of PRKAA1 was determined. Eca-109 and TE-1 cells were transfected with miR-NC, miR-940, miR-940 + vector and miR-940+ PRKAA1, (b–d) proliferation, (e–g) cell cycle and apoptosis, (h) PCNA, cyclin D1 and cleaved caspase 3 protein levels, (i) caspase-3 activity, (j and k) migration and invasion (l) angiogenesis were detected. *p < 0.05

FIGURE 8 PRKAA1 protein level was coregulated by miR-940 and circ_0003340. (a and b) PRKAA1 protein level was measured using western blot in Eca-109 and TE-1 cells transfected with si-NC, si-circ_0003340, si-circ_0003340 + anti-miR-NC, si-circ_0003340 + anti-miR-940. *p < 0.05
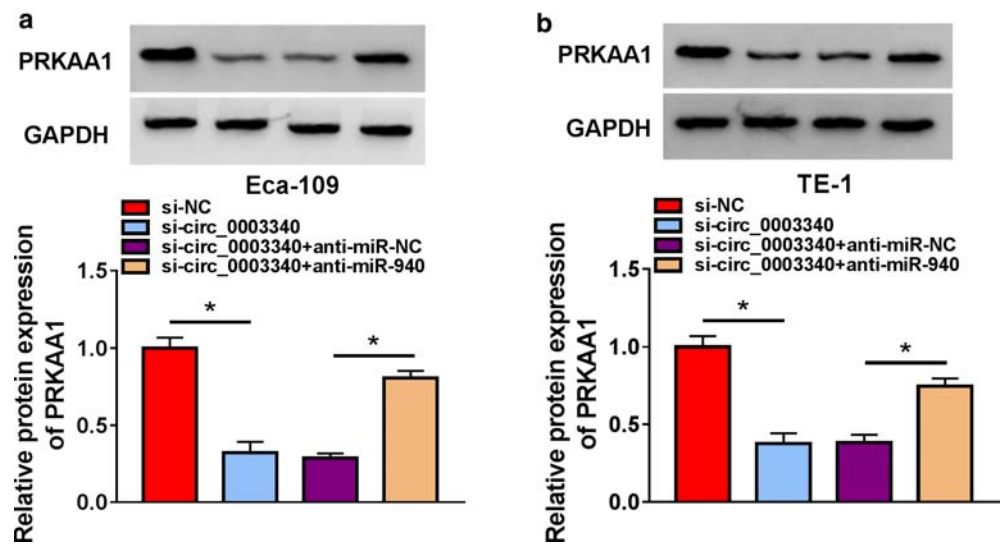
Circ_0003340 knockdown slowed tumor growth in vivo

Animal models were constructed by injecting Eca-109 cells stably transfected with sh-circ_0003340 or sh-NC into the nude mice, and we found that the tumor volume and weight of mice in which injected Eca-109 cells were stably transfected with sh-circ_0003340 were smaller and lighter (Figure 9a–c). Furthermore, we found that the levels of circ_0003340 and PRKAA1 were lower and miR-940 was higher in the tumor tissues of mice in which injected Eca-109 cells were stably transfected with sh-circ_0003340

compared to sh-NC (Figure 9d–f). Finally, the inhibition of the proliferation marker Ki67 level in mouse tumor tissues by sh-circ_0003340 was also demonstrated by IHC assay (Figure 9g). To conclude, circ_0003340 knockdown curbed tumor growth in vivo.

DISCUSSION

Currently, accumulating evidence has revealed the important regulatory potential of circRNAs in cancer. Many circRNAs have been observed to be dysregulated in ESCC. For
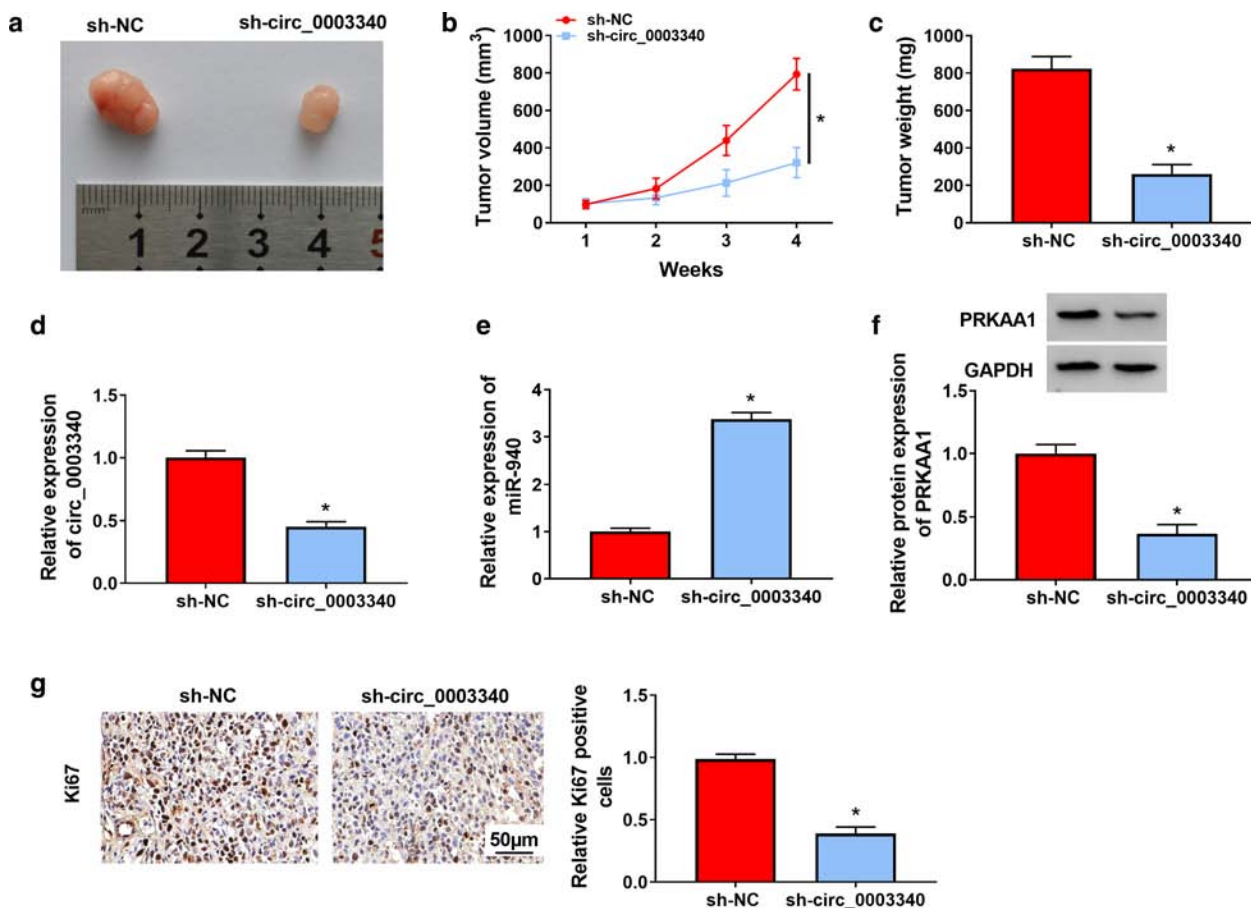
FIGURE 9 Effect of circ_0003340 on tumor growth in mice in vivo. (a) Representative images of tumor tissues were shown. (b) Tumor tissues were weighed. (c) Tumor tissue volume was measured. (d–f) Circ_0003340, miR-940 and PRKAA1 levels in tumor tissues were analyzed. (g) Ki67 content in tumor tissues was measured by IHC assay. *$p < 0.05$

example, in a recent study, the high expression of circ-SLC7A5 in plasma was found to be notably associated with TNM stage and survival of patients.[23] Circ_0058063 was also determined to have a higher abundance in ESCC, while circ_0058063 upregulation increased glucose uptake and cell proliferation, with the opposite result for circ_0058063 knockdown, showing the side effects of circ_0058063 in ESCC.[24] Circ_0003340 has previously been shown to be dysregulated in ESCC and facilitated ESCC cell proliferation, migration and invasion, and arrested apoptosis.[25] Angiogenesis is an important basis for tumor cell proliferation and metastasis, and the development of antiangiogenic drugs has become a hot spot in cancer research.[26] Our study identified a high abundance of circ_0003340 in ESCC, and found that knockdown of circ_0003340 notably restrained ESCC cell proliferation, migration, invasion and tube formation, but enhanced apoptosis. Moreover, circ_0003340 silencing also curbed tumor growth in vivo. Hence, circ_0003340 may be a promising therapeutic target for ESCC.

MiRNAs are central members of the ceRNA machinery. CircRNAs have been reported to act as miRNA sponges to regulate downstream gene levels, which has become a very common physiological or pathological regulatory

mechanism.[27] The dysregulation of miRNAs has also been established in ESCC, and abundant miRNAs have been discovered, such as miR-181b-5p. This has been found to be dramatically upregulated in ESCC and strongly associated with poorer survival rates in patients.[28] Our study detected a substantial downregulation of miR-940 in ESCC tissues and cells, while miR-940 overexpression had distinct proliferation, metastasis and angiogenesis inhibitory and apoptosis promoting effects. MiR-940 has regulatory roles in other cancer types, such as in hepatocellular carcinoma (HCC), and miR-940 has been identified as a differentially expressed gene. MiR-940 upregulation has also been reported to have a strong blocking effect on HCC progression both in vivo and in vitro.[29] Our study enriched the function of miR-940 in various diseases and refined the molecular regulatory network in ESCC.

In our study, PRKAA1 was shown to be a downstream regulatory molecule of miR-940. It was also detected to be prominently upregulated in ESCC, and to be involved in ESCC progression regulation. PRKAA1 had been widely studied in various diseases. Yang et al. revealed that PRKAA1 plays a regulatory role in atherosclerotic diseases, and PRKAA1 knockdown suppresses glycolytic pathways

and endothelial cell viability, in turn aggravating the disease.[30] In gestational diabetes, PRKAA1 displayed lower expression and PRKAA1 level affected inflammatory responses and cell viability.[31] Our study indicated an association between PRKAA1 and ESCC cell proliferation, metastasis and angiogenesis, and confirmed that circ_0003340 downregulation mitigated ESCC progression by targeting miR-940/PRKAA1 axis. In conclusion, our research provides promising targets for the diagnosis and treatment of ESCC.

CONFLICT OF INTEREST
The authors declare that they have no conflicts of interest.

ORCID
Hongjun Xu https://orcid.org/0000-0002-1363-5908

REFERENCES
1. Fitzmaurice C, Abate D, Abbasi N, Abbastabar H, Allah FA, Rahman OA, et al. Global, regional, and National Cancer Incidence, mortality, years of life lost, years lived with disability, and disability-adjusted life-years for 29 cancer groups, 1990 to 2016: a systematic analysis for the global burden of disease study. JAMA Oncol. 2018;4:1553–68.
2. Abnet CC, Arnold M, Wei WQ. Epidemiology of esophageal squamous cell carcinoma. Gastroenterology. 2018;154:360–73.
3. Engel LS, Chow WH, Vaughan TL, Gammon MD, Risch HA, Stanford JL, et al. Population attributable risks of esophageal and gastric cancers. J Natl Cancer Inst. 2003;95:1404–13.
4. Reichenbach ZW, Murray MG, Saxena R, Farkas D, Karassik EG, Klochkova A, et al. Clinical and translational advances in esophageal squamous cell carcinoma. Adv Cancer Res. 2019;144:95–135.
5. Torre LA, Siegel RL, Ward EM, Jemal A. Global cancer incidence and mortality rates and trends–an update. Cancer Epidemiol Biomarkers Prev. 2016;25:16–27.
6. Harada K, Rogers JE, Iwatsuki M, Yamashita K, Baba H, Ajani JA. Recent advances in treating oesophageal cancer. F1000Res. 2020;9:1189.
7. Cocquerelle C, Mascrez B, Hetuin D, Bailleul B. Mis-splicing yields circular RNA molecules. FASEB J. 1993;7:155–60.
8. Zhang HD, Jiang LH, Sun DW, Hou JC, Ji ZL. CircRNA: a novel type of biomarker for cancer. Breast Cancer. 2018;25:1–7.
9. Li P, Chen S, Chen H, Mo X, Li T, Shao Y, et al. Using circular RNA as a novel type of biomarker in the screening of gastric cancer. Clin Chim Acta. 2015;444:132–6.
10. Hong W, Xue M, Jiang J, Zhang Y, Gao X. Circular RNA circ-CPA4/let-7 miRNA/PD-L1 axis regulates cell growth, stemness, drug resistance and immune evasion in non-small cell lung cancer (NSCLC). J Exp Clin Cancer Res. 2020;39:149.
11. Guo J, Chen M, Ai G, Mao W, Li H, Zhou J. Hsa_circ_0023404 enhances cervical cancer metastasis and chemoresistance through VEGFA and autophagy signaling by sponging miR-5047. Biomed Pharmacother. 2019;115:108957.
12. Li T, Sun X, Chen L. Exosome circ_0044516 promotes prostate cancer cell proliferation and metastasis as a potential biomarker. J Cell Biochem. 2020;121:2118–26.
13. Hou Y, Liu H, Pan W. Knockdown of circ_0003340 induces cell apoptosis, inhibits invasion and proliferation through miR-564/TPX2 in esophageal cancer cells. Exp Cell Res. 2020;394:112142.
14. Landgraf P, Rusu M, Sheridan R, Sewer A, Iovino N, Aravin A, et al. A mammalian microRNA expression atlas based on small RNA library sequencing. Cell. 2007;129:1401–14.
15. Bartel DP. Metazoan MicroRNAs. Cell. 2018;173:20–51.
16. Mamoori A, Gopalan V, Lam AK. Role of miR-193a in cancer: complexity and factors control the pattern of its expression. Curr Cancer Drug Targets. 2018;18:618–28.
17. Pekow J, Meckel K, Dougherty U, Huang Y, Chen X, Almoghrabi A, et al. miR-193a-3p is a key tumor suppressor in ulcerative colitis-associated colon cancer and promotes carcinogenesis through upregulation of IL17RD. Clin Cancer Res. 2017;23:5281–91.
18. Zhou DD, Li HL, Liu W, Zhang LP, Zheng Q, Bai J, et al. miR-193a-3p promotes the invasion, migration, and mesenchymal transition in glioma through regulating BTRC. Biomed Res Int. 2021;2021:8928509.
19. Wang H, Song T, Qiao Y, Sun J. miR-940 inhibits cell proliferation and promotes apoptosis in esophageal squamous cell carcinoma cells and is associated with post-operative prognosis. Exp Ther Med. 2020;19:833–40.
20. Gleason CE, Lu D, Witters LA, Newgard CB, Birnbaum MJ. The role of AMPK and mTOR in nutrient sensing in pancreatic beta-cells. J Biol Chem. 2007;282:10341–51.
21. Green AS, Chapuis N, Lacombe C, Mayeux P, Bouscary D, Tamburini J. LKB1/AMPK/mTOR signaling pathway in hematological malignancies: from metabolism to cancer cell biology. Cell Cycle. 2011;10:2115–20.
22. Zhang Y, Zhou X, Zhang Q, Zhang Y, Wang X, Cheng L. Involvement of NF-κB signaling pathway in the regulation of PRKAA1-mediated tumorigenesis in gastric cancer. Artif Cells Nanomed Biotechnol. 2019;47:3677–86.
23. Wang Q, Liu H, Liu Z, Yang L, Zhou J, Cao X, et al. Circ-SLC7A5, a potential prognostic circulating biomarker for detection of ESCC. Cancer Genet. 2020;240:33–9.
24. Zheng Y, Chen Y, Jiang H, Zhang H, Wang H, Xu J, et al. Circ_0058063 upregulates GLUT1 expression and promotes glucose-uptake in esophageal squamous-cell carcinomas. J Thorac Dis. 2020;12:925–31.
25. Liang Z, Zhao B, Hou J, Zheng J, Xin G. CircRNA circ-OGDH (hsa_circ_0003340) acts as a ceRNA to regulate glutamine metabolism and esophageal squamous cell carcinoma progression by the miR-615-5p/PDX1 Axis. Cancer Manag Res. 2021;13:3041–53.
26. Lv T, Zhao Y, Jiang X, Yuan H, Wang H, Cui X, et al. uPAR: an essential factor for tumor development. J Cancer. 2021;12:7026–40.
27. Abdollahzadeh R, Daraei A, Mansoori Y, Sepahvand M, Amoli MM, Tavakkoly-Bazzaz J. Competing endogenous RNA (ceRNA) cross talk and language in ceRNA regulatory networks: a new look at hallmarks of breast cancer. J Cell Physiol. 2019;234:10080–100.
28. Wang Y, Lu J, Chen L, Bian H, Hu J, Li D, et al. Tumor-derived EV-encapsulated miR-181b-5p induces angiogenesis to Foster tumorigenesis and metastasis of ESCC. Mol Ther Nucl Acids. 2020;20:421–37.
29. Li P, Xiao Z, Luo J, Zhang Y, Lin L. MiR-139-5p, miR-940 and miR-193a-5p inhibit the growth of hepatocellular carcinoma by targeting SPOCK1. J Cell Mol Med. 2019;23:2475–88.
30. Yang Q, Xu J, Ma Q, Liu Z, Sudhahar V, Cao Y, et al. PRKAA1/AMPKα1-driven glycolysis in endothelial cells exposed to disturbed flow protects against atherosclerosis. Nat Commun. 2018;9:4667.
31. Peng HY, Li MQ, Li HP. High glucose suppresses the viability and proliferation of HTR-8/SVneo cells through regulation of the miR-137/PRKAA1/IL-6 axis. Int J Mol Med. 2018;42:799–810.